

INFLUENCES OF FINISHED GEOMETRY OF SPECIMEN FOR COMPRESSION TEST ON THE STABILITY OF TESTING AND PRECISION OF MEASURED STRESS AND STRAIN

JUNKI MIYAGAWA^{*}, SHIGERU OHBA[†], MASAYOSHI AKIYAMA^{††}

^{*} Taisei Kako Co., Ltd.
2-11-12, Fujinosato, Ibaraki city, Osaka 567-0054, Japan
e-mail: ewhfocenj@yahoo.co.jp, web page: www.taisei-g.co.jp

[†] Sumitomo Metals Technology Ltd. 1-8 Fuso-cho, Amagasaki, 660-0891, Japan
e-mail: ooba-sgr@smt-co.jp

^{††} Department of Mechanical and System Engineering, Kyoto Institute of Technology (KIT)
Goshokaido-cho, Matsugasaki, Sakyo-ku, Kyoto, 606-8585, Japan
email: akiyama@mech.kit.ac.jp, web page: www.mesh.kit.ac.jp

Key words: Compression Test, Cylinder, ASTM-E9 89a, Precision, Stress-Strain Curve.

Abstract. This paper deals with the influence of the specimen geometry on the precision of measured stress-strain curve on the compression side. Cylindrical specimen is adopted after ASTM-E9 89a and laboratory experiment and elastic-plastic FEA are carried out to evaluate the influence of the degree of parallelism of end surfaces. Present tolerance value of 0.5/1000 for the inclination of end surface can be relieved up to 6/1000.

1 INTRODUCTION

Stress-strain curve is an essential characteristic when one analyzes the plastic deformation of a material. Usually only a tension test is carried out to know the stress-strain curve on an assumption such that the stress-strain curve is point symmetric around the origin. This assumption is approximately correct, but in an exact sense two curves are slightly different [1]. If the difference is not negligibly small the assumption of point symmetry may lead to a discrepancy between the experimental and analytical results and prediction by the analysis of the forming process fails. For the prevention of this failure one ought to carry out a compression test as well as the tension test prior to the analysis [2]. Compression test specified by ASTM-E9 89a [3] is a commonly used compression test. For this test a cylindrical specimen is prepared in a manner such that the degree of parallelism of end surfaces must lie within the tolerance value of 0.5/1000, although the background of this tolerance value is not clear. If it is possible to loosen the tolerance value it will help specimen preparation. In the following part of this paper experiments and numerical analyses are carried out to evaluate the influence of specimen geometry on the precision of measured stress and strain and expansion of tolerance value is discussed. The code for numerical analysis is ELFEN [4] developed at University of Swansea, U.K.

2 PREPARATIONS

2.1 Specimen preparations

Figure 1 shows the manufacturing process for specimen. Parent bar was subjected to turning after thermal treatment at 680°C and the end surface was finished by a sandpaper.

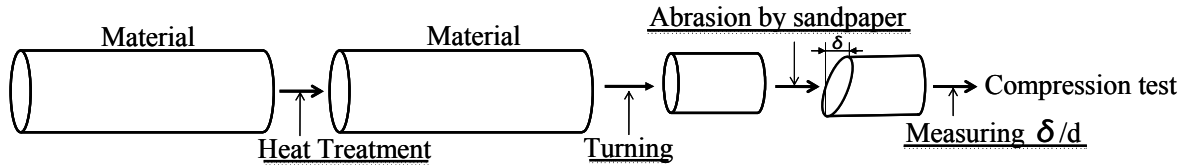


Figure 1: Flow of processing for preparing specimen for compression test

2.2 Theory

Inclination of end surface was measured by using the following theory. It was assumed that both end surfaces were flat planes and one end surface that was exactly perpendicular to the axis was placed on a flat table that was spanned by X and Y axes as is illustrated in Figure 2. The plane showing the top flat surface may cross the X-Y-plane, and the inclination angle α and parallelism (δ/d) of the top flat surface is calculated by determining the line AB.

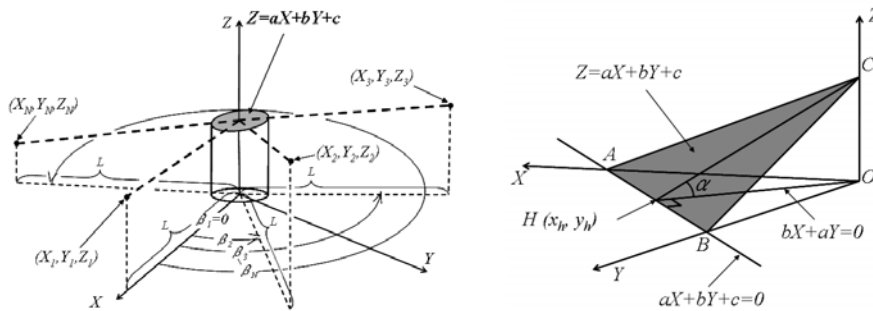


Figure 2: Illustrated image for measuring geometry of inclined upper surface

The equation of top flat surface is given by equation (1). Using the least square method the constants a , b and c are calculated, i.e. minimization process of the error S given by equation (2) leads to a set of equations (3), (4) and (5). Precise measurement of N sets of coordinate values (X_i, Y_i, Z_i) determines the plane ABC, where N must be larger than 2.

$$Z = aX + bY + c \quad (1)$$

$$S = \sum_{i=1}^N (Z_i - aX_i - bY_i - c)^2 \quad (2)$$

$$\frac{\partial S}{\partial a} = 0 \quad (3)$$

$$\frac{\partial S}{\partial b} = 0 \quad (4)$$

$$\frac{\partial S}{\partial c} = 0 \quad (5)$$

Once a, b and c are determined the coordinate values of (X_h, Y_h) of point H are calculated by solving a set of equations (6) and (7). The inclination angle α of the top flat surface is then calculated by using equation (8) and the parallelism (δ/d) is also calculated.

$$aX + bY + c = 0 \quad (6)$$

$$bX - aY = 0 \quad (7)$$

$$\alpha = \tan^{-1}\left(\frac{OC}{OH}\right) \quad (8)$$

2.3 Measurement

Figure 3 shows the outline of the measuring system. Coordinate values of (X_i, Y_i) of each data points were calculated according to the angle β_i and the fixed length L and the value Z_i was the height of the spot of a laser pointer mounted on the top flat surface of the specimen.

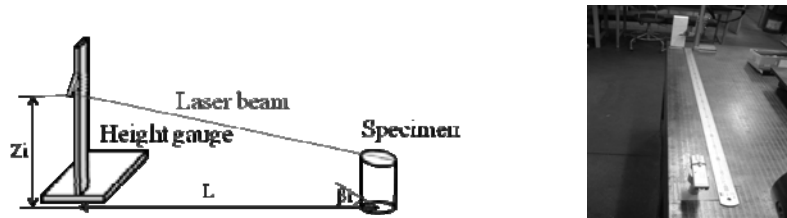


Figure 3: Illustration and view of measuring height of laser spot Z_i

2.4 Result

Table 1 shows the measured values of parallelism of specimens. The range of parallelism lies between naught and 50/1000, and plural number of specimens were prepared for each geometrical conditions in Table 1.

Table 1: Calculated degree of inclination angle α of specimen

Specimen number	1	2	3	4	5	6	7	8
Parallelism of end surface (δ/d)	1/1000	2/1000	6/1000	7/1000	15/1000	23/1000	40/1000	48/1000

2.5 Tooling

A protector and a set of toolings for compression test were manufactured as shown in Figure 4. Compression test may endanger the operator because the specimen can suddenly become a bullet, and the protector prevents this danger from occurring. On the side of the protector there is a hole that is smaller than the specimen size and the cables from strain gauges placed on the specimen are drawn through this hole. The material of toolings was 0.45 mass % carbon steel and was prepared according to the thermal treatment illustrated in Figure 5 [5].

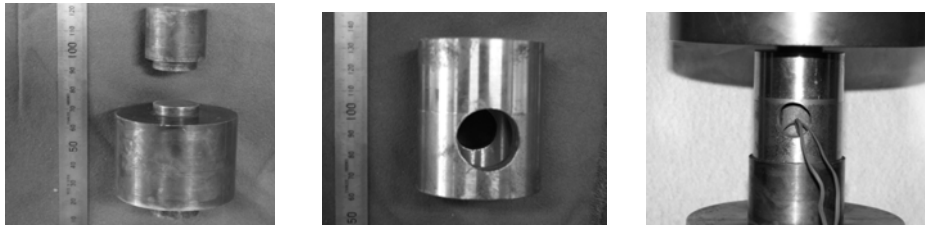


Figure 4: Tooling and protector for compression test

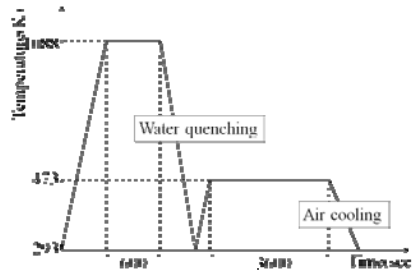


Figure 5: Diagram for quenching and tempering operations for toolings

3 EXPERIMENT

Compression test was carried out using a universal testing machine shown in Figure 6. The aspect ratio of specimens was 2.5 following the previous work on the uniformity of measured stress and strain in compression test [6,7]. Test was conducted until 5% strain was reached. Strain was measured by using four strain gauges placed at the specimen centre in a pitch of 90 degrees. Stress was a nominal stress. Cross head speed was 1mm/min.

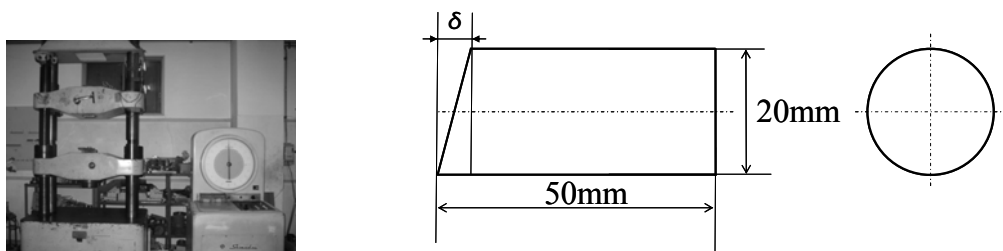


Figure 6: Machine and prepared specimen for compression test

Lubricant was prepared according to the previous work [8,9]. Soap mixed with powdered mild detergent for washing was placed on the specimen surface prior to the test.



Figure 7: View of lubricant

4 RESULT

4.1 Stability of experiment

No specimen flew as a bullet and the compression test was stable, but buckling occurred in accordance with the increase the index of parallelism (δ/d). Examples of normal and buckled specimens are shown in Fig. 8. All the specimens were observed under the back light after the test and the specimen was esteemed buckled when an opening was observed.

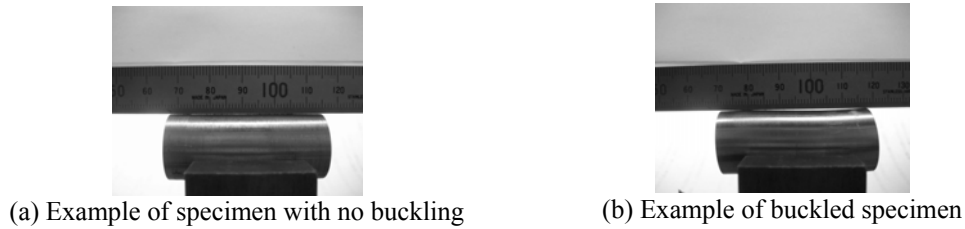


Figure 8: Comparison of non-buckled and buckled specimens

Figure 9 shows the influence of the index of parallelism (δ/d) on buckling. Ordinate is the buckling index. The buckling index is 1 when buckling occurs on all the specimens and 0.5 when buckling occurs on 50% specimens and 0 when no buckling occurs. The critical value of the index of parallelism (δ/d) may be 7/1000 above which buckling occurs.

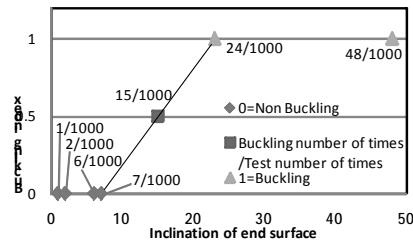


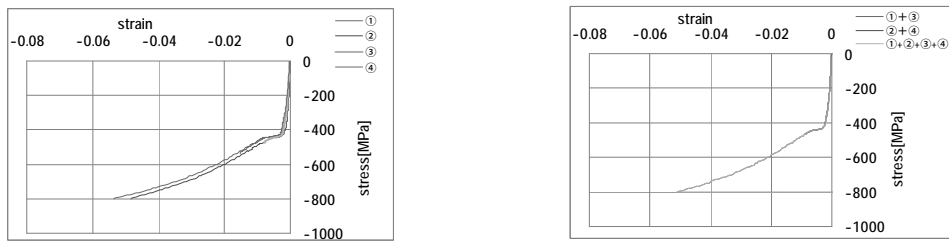
Figure 9: Influence of inclination of end surface upon on buckling

4.2 Stress-strain curves

Figure 10 shows the positions of four strain gauges placed in the circumferential direction at the specimen centre. No-1 gauge was placed on the longest portion of specimen and No-3 gauge on the shortest portion. Examples of four stress-strain curves are drawn in Figure 11. They were drawn by using the signals of four gauges, and three curves in Figure 11b are drawn by using the average strains. Three stress-strain curves in Figure 11b are almost the same and it can be recommended to take an average value of measured strains.



Figure 10: Illustrated image of placement of strain gauges



(a) Example of stress-strain curves for four strains (Inclination 6/1000) (b) Comparison of average stress-strain curves on opposite angle (Inclination 6/1000)

Figure 11: Influence of inclination of end surface upon on stress-strain curves

The tangents of elastic region of stress-strain curves in Figure 11a lie in a wide range and it is unrealistic. However the tangents in Figure 11b measured within the stress range of -200 and -300MPa was a reasonable value of 206GPa.

Figure 12 is a comparison of stress-strain curves among specimens with different value of the index of parallelism (δ/d). It may be concluded that difference in the index of parallelism does not seriously influence the measured stress-strain curve as long as the value of index lies within the range of under (6/1000).

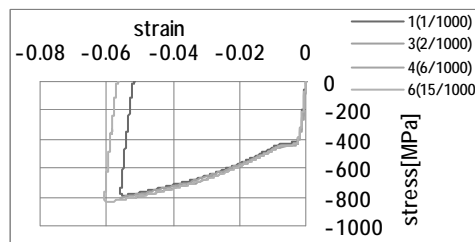


Figure 12: Comparison of raw stress-strain curves for all none buckling specimens

5 NUMERICAL ANALYSIS

5.1 Conditions for analysis

In order to examine the precision of measured stress and strains elastic-plastic FEA were carried out on the compression tests. The stress-strain curve was that given in Figure 11b. The stress-strain curve was assumed point-symmetric on the tension side. The parameter changed in the analyses was the inclination index δ of the end surface in Figure 6 and the response of specimen was examined.

Figure 13 shows an example of 3D initial mesh for the analysis. The centre portion was divided into 6 times 6 small squares. The outside layer was divided into 5 thin layers and the division in the circumferential direction was 24. The mesh division in a cross section was 156. The mesh division in the longitudinal direction was 24, and the total number of elements was 3744. Displacement constraint was given in the axial direction on all the nodes on the lower end surface and upper surface was compressed by a rigid ram as shown in Figure 14.

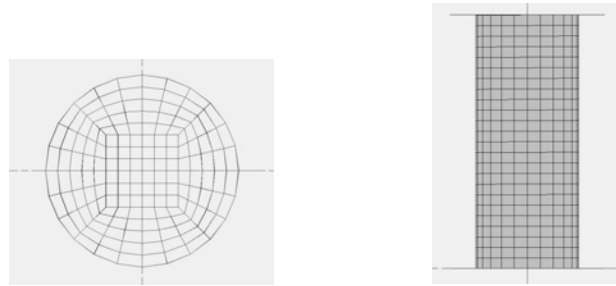


Figure 13: Illustrated image of dividing mesh

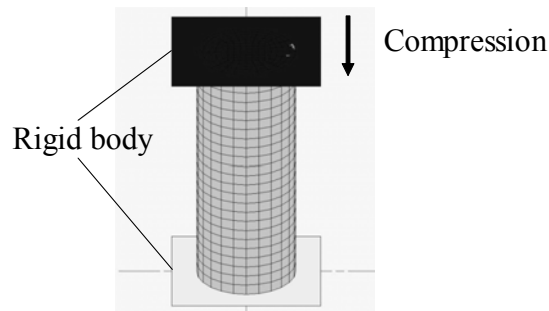


Figure 14: Loading procedure

5.2 Distribution of stress

Figure 15 shows examples of distribution of axial stress on the elastic and plastic stages for a specimen with the index (δ/d) of 6/1000 on the centre plane of specimen. On the elastic stage, there is a clear distribution of stress according to the inclination of end surface, but it gradually fades out on the plastic stage. The average value of stress is equal to the compressive force divided by the cross sectional area of the centre plane.



(a) Elastic stage (0.18% compression)

(a) plastic stage (1.5% compression)

Figure 15: Examples of stress distributions on elastic and plastic stages

5.3 Distribution of strain

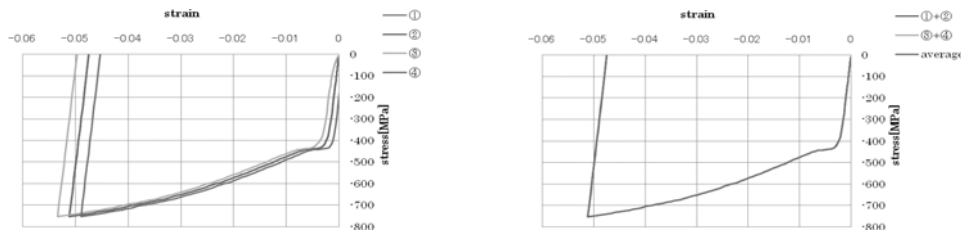
Figure 16 shows examples of distribution of axial strain on the centre plane of the specimen on the elastic and plastic stages. Figure 18-(a) and (b) show the distributions on the elastic and plastic stages respectively. Similarly to the distribution of axial stress distribution of axial strain on the elastic stage is slightly large but it gradually fades out on the plastic stage. There is also a distribution of other strain components but the intensity of those components is much smaller than that of the axial strain.



(a) Elastic stage (0.18% compression) (b) Elastic stage (1.5% compression)
Figure 16: Comparison of Distribution of strain in elastic stage and plastic stage

5.4 Stress-strain curve

Figure 17 shows four stress-strain curves drawn for each calculated stress and strain on the four points placed in the same pitch of 90 degrees around the specimen corresponding to the measuring points of strain in the compression test in a laboratory. As was expected four stress-strain curves on the elastic stage are totally different, but those are nearly the same on the plastic stage. Three average stress-strain curves drawn by using the average value of two strains all the four strains show an excellent matching one another. The Young's modulus of the average stress-strain curves sampled within the stress range of -200 and -300 MPa was 201GPa.



(a) Comparison of four stress-strain curves (b) Comparison of average stress-strain curves
Figure 17: Comparison of average stress-strain curves (Inclination 6/1000)

Figure 18 is a comparison between the analytical and measured stress-strain curves on the compression side. The material is a medium carbon steel with 0.45 mass % carbon content. Good agreement has been achieved and it may be concluded that by taking the average value of at least two strains around the circumferential direction of specimen. Especially excellent matching is obtainable when the stress state is plastic.

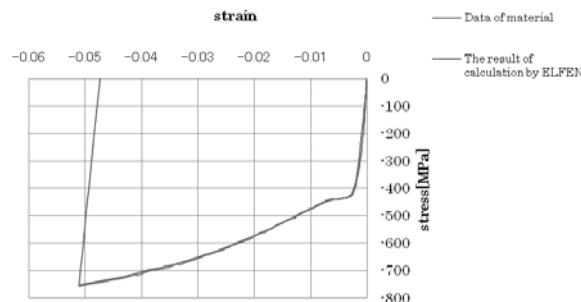


Figure 18: Comparison of result of experiment and numerical analysis

6 CONCLUSIONS

In the present work influence of parallelism of end surfaces on specimen for compression test on the precision of stress-strain curve on the compression side was evaluated numerically and experimentally. None of the specimens of which parallelism ranged from 1/1000 to 48/1000 suddenly flew as a bullet throughout the test, but buckling was observed when the parallelism exceeded 7/1000. If average strain is adopted on the centre plane of the cylindrical specimen the stress-strain curve obtained is almost the same as the true stress-strain curve of the material. The number of signals of strain should be at least two that face each other in the circumferential direction in a pitch of 180 degrees. If the number is four by placing the strain gauge in a pitch of 90 degrees, stress-strain curve drawn by using this average strain is exactly the same as the true stress-strain curve. It is specified in ASTM E9-89a that the parallelism of end surfaces must lie within a range of 0.5/1000, but this specified value can be until 6/1000 as long as the strain is measured in the circumferential direction on the centre plane in the same pitch of 90 or 180 degrees. In the present work influence of parallelism of end surfaces on specimen for compression test on the precision of stress-strain curve on the compression side was evaluated numerically.

ACKNOWLEDGEMENT

This project was carried out with the financial assistance of The Amada Foundation, Japan, and the authors would like to express their deep gratitude for the support.

REFERENCES

- [1] Shinji Fukui, Hideaki Kudo, Kiyota Yoshida, and Kunio Abe. Methods of Obtaining the Stress-Strain Curves of Ductile Metals for Large Strain Region, *The reports of the Institute of Science and Technology*, The University of Tokyo, No.8, Vol.3 (1954), pp.135-151.
- [2] M. Akiyama, Proposal of a project for the prediction of anisotropy, *ISO TC67/SC5*, Washington, U.S.A., (2004).
- [3] ASTM International, *Designation: E9-89a* (Reapproved 2000), pp.90-98.
- [4] Rockfield Software Limited, URL: www.rockfield.co.uk
- [5] Toru Araki, Heat-treatment Technology of Steel(in Japanese), *Vol. 8 of Lecture Series on Iron and Steel Engineering*, Asakura Publishing Co., Ltd, (1969), pp.1-20.
- [6] Atsushi Ichijo, Masayoshi Akiyama, Numerical Re-examination of Simple Compression Test, *Proceedings of COMPLAS X*, (2009).
- [7] Atsushi ICHIJO, Masayoshi AKIYAMA. Precision of Measured Stress and Strain in Compression Test for Cylindrical Specimen, *to be published in SOSEI-TO-KAKOU. J. of The Japan Society for Technology of Plasticity, Vol.52, no. 604*, (2011-5).
- [8] Hiroshi Ohyama, Masayoshi Akiyama, Evaluation of Environment-Friendly Lubricant by Erichsen Test, *Proceedings of COMPLAS X*, (2009).
- [9] Hiroshi OHYAMA, Masayoshi AKIYAMA. Development and Evaluation of Environmentally Friendly Lubricant for Cold metal Working, *SOSEI-TO-KAKOU. J. of The Japan Society for Technology of Plasticity, Vol.52, no.603*, (2011-4), pp.474-479.